Research Article

Pre-clinical study of human umbilical cord mesenchymal stem cell transplantation for the treatment of traumatic brain injury: safety evaluation from immunogenic and oncogenic perspectives

https://doi.org/10.4103/1673-5374.317985
Date of submission: July 19, 2020
Date of decision: September 10, 2020
Date of acceptance: April 12, 2021
Date of web publication: July 8, 2021

Gang Wang[1, 2, #], Hua-Ling Wu[3, #], Yue-Ping Liu[1, 2, #], De-Qi Yan[4], Zi-Lin Yuan[1, 2], Li Chen[1, 2], Qian Yang[1, 2], Yu-Song Gao[4], Bo Diao[1, 2, *]

Graphical Abstract *Human umbilical cord mesenchymal stem cells exhibit good immunomodulatory function*

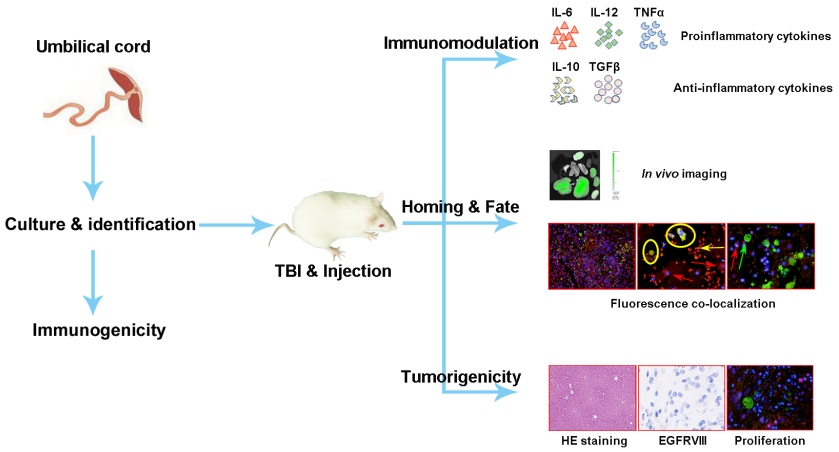

Abstract

Stem cell therapy is a promising strategy for the treatment of traumatic brain injury (TBI). However, animal experiments are needed to evaluate safety; in particular, to examine the immunogenicity and tumorigenicity of human umbilical cord mesenchymal stem cells (huMSCs) before clinical application. In this study, huMSCs were harvested from human amniotic membrane and umbilical cord vascular tissue. A rat model of TBI was established using the controlled cortical impact method. Starting from the third day after injury, the rats were injected with 10 μL of 5 × 10^6/mL huMSCs by cerebral stereotaxis or with 500 μL of 1 × 10^6/mL huMSCs via the tail vein for 3 successive days. huMSC transplantation decreased the serum levels of proinflammatory cytokines in rats with TBI and increased the serum levels of anti-inflammatory cytokines, thereby exhibiting good immunoregulatory function. The transplanted huMSCs were distributed in the liver, lung and brain injury sites. No abnormal proliferation or tumorigenesis was found in these organs up to 12 months after transplantation. The transplanted huMSCs negligibly proliferated *in vivo*, and apoptosis was gradually observed at later stages. These findings suggest that huMSC transplantation for the treatment of traumatic brain injury displays good safety. In addition, huMSCs exhibit good immunoregulatory function, which can help prevent and reduce secondary brain injury caused by the rapid release of inflammatory factors after TBI. This study was approved by the Ethics Committee of Wuhan General Hospital of PLA (approval No. 20160054) on November 1, 2016.

Key Words: cell transplantation; immune regulation; inflammation; mesenchymal stem cells; safety evaluation; immunogenicity; traumatic brain injury; tumorigenesis

Chinese Library Classification No. R456; R741.05; R318

Introduction

Although much has been learned about the cellular and molecular mechanisms of traumatic brain injury (TBI) in the past two decades, these advances have failed to translate into a successful clinical trial; thus, no therapies are currently available to effectively treat TBI (Saatman et al., 2008; Schepici et al., 2020). Because of their capacity to differentiate into neuronal cells and release neurotrophic factors, stem cell

[1]Basic Medical Laboratory, General Hospital of the Central Theater Command, Wuhan, Hubei Province, China; [2]Hubei Key Laboratory of Central Nervous System Tumor and Intervention, Wuhan, Hubei Province, China; [3]Department of Clinical Laboratory, The Third People's Hospital of Yongzhou, Yongzhou, Hunan Province, China; [4]Department of Neurosurgery, 990th Hospital of Joint Logistic Support Troops of PLA, Zhumadian, Henan Province, China
*Correspondence to: Bo Diao, MD, dpitao@163.com.
https://orcid.org/0000-0002-2209-6061 (Bo Diao)
#These authors contributed equally to this work.

Funding: *The work was supported by the General Project of Hubei Health Committee of China, No. WJ2019M263 (to GW).*
How to cite this article: *Wang G, Wu HL, Liu YP, Yan DQ, Yuan ZL, Chen L, Yang Q, Gao YS, Diao B (2022) Pre-clinical study of human umbilical cord mesenchymal stem cell transplantation for the treatment of traumatic brain injury: safety evaluation from immunogenic and oncogenic perspectives. Neural Regen Res 17(2):354-361.*

therapy is a promising therapeutic strategy for TBI (Schepici et al., 2020).

Recent stem cell-based therapies, which use sources such as bone marrow mesenchymal stem cells (MSCs) (Lam et al., 2017; Yuan et al., 2021), human umbilical cord MSCs (huMSCs) (Shi et al., 2012), oligodendrocyte progenitor cells (Xu et al., 2015), neural stem cells (Gao et al., 2016; Liu et al., 2021) and neural progenitor cells (Blaya et al., 2015), have been reported to be beneficial in treating TBI. However, because of their allogenicity and their proliferative similarity to tumor cells, questions remain regarding immunological rejection reactions, tumorigenesis and uncontrolled proliferation of stem cells, which could cause sudden onset of glioblastoma after TBI (Tyagi et al., 2016), especially when MSCs are used in glioma patients (Nakamura et al., 2004). These challenges have delayed the application of stem cells in the clinical treatment of TBI. Furthermore, a previous study identified two distinct mesenchymal stromal cell populations in human malignant glioma (Svensson et al., 2017). Therefore, animal experiments are necessary to evaluate the safety of huMSC transplantation prior to clinical application.

Here, we first isolated and immunophenotypically characterized huMSCs. The huMSCs were then transplanted into experimental animals *in situ* or via the tail vein. A safety evaluation study was conducted of the immunogenicity, immunomodulatory effects, tumorigenesis and main organ distribution of the transplanted huMSCs in the rat model of TBI. The immunogenic and immunomodulatory effects of huMSCs were evaluated by detection of human leukocyte antigen II (HLAII) and serum pro-inflammatory and anti-inflammatory cytokines.

Materials and Methods

HuMSC isolation and identification

All procedures for umbilical cord collection and manipulation were performed in accordance with the regulations of the Ethics Committee of Wuhan General Hospital of PLA, and this study was approved by the review board (approval No. 20160054) on November 1, 2016. After obtaining informed consent from the donor, fresh amniotic membrane and umbilical cord vascular tissue were cut into 1-mm^3 pieces with ophthalmic scissors and placed into sterile dishes. StemPro MSC SFM XenoFree (Gibco, Grand Island, NY, USA) culture medium was added into the dish, which was gently shaken to promote even mixing, and transferred into a 5% CO_2/37°C incubator (Thermo Scientific, Waltham, MA, USA). Half of the culture medium was replaced every 5 days. On day 10, long spindle-like cells were observed growing from the edge of the tissue block. On day 14, when the cells covered 50% of the surface area, the tissue blocks were removed, and the cells were collected for continuous culture. The culture medium was replaced every 3 days. When cells reached 90% confluence, 0.25% trypsin was used to detach the cells. The suspended cells were incubated for 1 hour at room temperature in the dark with fluorescent antibodies (anti-CD29-APC, anti-CD44-PE, anti-CD73-PE and anti-CD105-APC; BD Bioscience, San Jose, CA, USA). Cells were then washed 3 times and analyzed using a FACSCalibur cytometer (Becton, Dickinson and Company, Franklin Lakes, NJ, USA). The huMSCs from the third passage were used in subsequent experiments.

Detection of huMSC HLAII expression by western blot and quantitative real-time polymerase chain reaction

HLAII expression was detected by western blot. First, 10 μg huMSC lysate was resolved on SDS-PAGE gels and transferred onto polyvinylidene difluoride membranes (Millipore, Bedford, MA, USA). After blocking in 5% skim milk for 30 minutes, the membranes were incubated with anti-major histocompatibility complex (MHC) Class II (HLAII) mouse monoclonal antibody (Cat# ab55152, 1:2000, Abcam, Cambridge, UK) or anti-glyceraldehyde 3-phosphate dehydrogenase (GAPDH) mouse monoclonal antibody (Cat# 60004-1-Ig, 1:5000, Proteintech, Wuhan, China) at 4°C overnight. After washing, the membranes were incubated with horseradish peroxidase-conjugated goat anti-mouse IgG (Cat# SA00001-1, 1:3000, Proteintech) at room temperature for 1 hour. After washing, the blots were developed using Pierce ECL western blotting substrate (Thermo Scientific) and then imaged and analyzed with the Tanon 5200 automatic chemiluminescence image analysis system (Tanon Company, Shanghai, China).

HLA-DPA1, *HLA-DQA1* and *HLA-DRA1* were selected from among the 16 human *HLAII* genes to assess their mRNA expression in huMSCs. Peripheral blood mononuclear cells were separated from human peripheral blood by density gradient centrifugation with Ficoll as a positive control. The GenBank mRNA sequences of *HLA-DPA1* (accession: NM_001242524.1), *HLA-DQA1* (accession: NM_002122.3), *HLA-DRA1* (accession: NM_019111.4) and *GAPDH* (accession: NM_001256799.2) were used to design primers for qRT-PCR. The following primers were used: *HLA-DPA1* forward: 5′-CTG GAC AAG AAG GAG ACC GT-3′; *HLA-DPA1* reverse: 5′-TCA ATG TGG CAG ATG AGG GT-3′ (product length 224 kb); *HLA-DQA1* forward: 5′-AAC GCT ACA ACT CTA CCG CT-3′; *HLA-DQA1* reverse: 5′-TCT GTG ACT GAC TGC CCA TT-3′ (product length 166 kb); *HLA-DRA1* forward: 5′-AAT GGC CAT AAG TGG AGT CC-3′; *HLA-DRA1* reverse: 5′-GGA GGT ACA TTG GTG ATC GG-3′ (product length 336 kb); *GAPDH* forward: 5′-CCA GAA CAT CAT CCC TGC CT-3′, *GAPDH* reverse: 5′-CCT GCT TCA CCA CCT TCT TG-3′ (product length 185 kb). Primers were synthesized by Tsingke Biological Technology (Wuhan, China). Total mRNA from huMSCs was extracted using TRIzol (Invitrogen, Carlsbad, CA, USA) and then reverse-transcribed into cDNA with a QuantiTect Reverse Transcription Kit (Qiagen, Hilden, Germany). The qRT-PCR mix was prepared with a Taq PCR MasterMix kit (TIANGEN, Beijing, China) according to the user guide and run on a LightCycler 96 (Roche, Basel, Switzerland).

HuMSCs labeled by carboxyfluorescein succinimidyl ester

HuMSCs were labeled using the CellTrace carboxyfluorescein succinimidyl ester (CFSE) Cell Proliferation Kit (Thermo Scientific) following the manufacturer's instructions. Briefly, huMSCs were suspended in prewarmed 0.1% bovine serum albumin-phosphate buffer saline (PBS) and CFSE. The cell concentration was 1×10^6/mL, and the CFSE concentration was 2.0 μM. The suspension was incubated for 15 minutes at 37°C in the dark. The staining was quenched by adding 5 volumes of ice-cold culture medium followed by incubation on ice for 5 minutes. Labeled cells were then washed with PBS three times and resuspended in 1×10^6/mL for tail vein injection and 5×10^6/mL for *in situ* brain injection.

Animal modeling, grouping and intervention

All Sprague–Dawley rats (Experimental Animal Center of Hubei Province, Wuhan, China, license No. SCXK-2015-0018) were housed according to the Guide for the Care and Use of Laboratory Animals of the National Academy of Sciences. All animal experiments were performed according to the animal study protocol approved by the Ethics Committee of Wuhan General Hospital of PLA (approval No. 20160054) on November 1, 2016. A total of 130 adult healthy Sprague–Dawley male rats (280–300 g, 8 weeks old) were fed a standard laboratory diet and water and maintained under temperature-controlled conditions (22 ± 2°C) and a 12-hour light/dark cycle. The rats were randomly distributed into the following four groups: sham, TBI model (TBI), *in situ* injected (*In Situ*), and tail vein injected (Tail Vein) groups.

Sham group (n = 25): The skin at the surgical site was cut open and then sutured. For detection, five rats were sacrificed at each time point in synchrony with the *In Situ* and Tail Vein groups.

TBI group (n = 25): The rat model of TBI was prepared using the Feeney method (Feeney et al., 1981). Briefly, animals were anesthetized with sodium pentobarbital (30 mg/kg, intraperitoneal injection; Sigma-Aldrich, St. Louis, MO, USA) and fixed on a cerebral stereotactic device (RuiWoDe, Shenzhen, China), and a craniotomy (4 mm × 4 mm) was performed above the right parietal cortex between the sagittal, lambdoid and coronal sutures. After removing the bone fragments from the dural surface, a 3 mm diameter impactor was employed to impact the dura at a speed of 2 m/s to cause traumatic brain injury. The impact depth was set at 2 mm to avoid dural breakdown. For detection, five rats were sacrificed at each time point in synchrony with the *In Situ* and the Tail Vein groups.

In Situ group (n = 40): On the third day after TBI, a single dose of 10 µL 5 × 10^6/mL CFSE-labeled cells was injected through the cerebral stereotactic device (RuiWoDe) with an aseptic microsyringe (Hamilton, Reno, NV, USA) to transplant the huMSCs into the brain injury impact site; the day after transplantation was considered day 1. For detection, five rats were sacrificed on days 1, 3, 7, 14 and 28. The remaining 15 rats were kept for an additional 12 months for long-term observation.

Tail Vein group (n = 40): After TBI, 500 µL of 1 × 10^6/mL CFSE-labeled cells was injected through the tail vein once per day for 3 days; the day after the last transplantation was considered day 1. For detection, five rats were sacrificed on days 1, 3, 7, 14 and 28. The remaining 15 rats were kept an additional 12 months for long-term observation.

Detection of serum cytokines by enzyme-linked immunosorbent assay

Serum was separated from the jugular blood collected on days 1, 3, 7, 14 and 28 from each group. The concentrations of the serum cytokines interleukin 6 (IL-6), interleukin 10 (IL-10) and interleukin 12 (IL-12), transforming growth factor beta (TGF-β) and tumor necrosis factor alpha (TNF-α) were measured using enzyme-linked immunosorbent assay (ELISA) kits. IL-6, IL-10, TGF-β and TNFα ELISA kits were purchased from Boster (Wuhan, China). The IL-12 ELISA Kit was purchased from Biorbyt Company (Cambridge, UK). All tests were conducted according to the manufacturers' instructions.

Localization of huMSCs by *in vivo* imaging

We examined the colonization pattern and metabolism of the CFSE-labeled transplanted huMSCs. The rats were sacrificed by decapitation after inhalation anesthesia with diethyl ether (Sinopharm Chemical Reagent Co., Ltd., Shanghai, China). After dissection, the brain, liver, lung, kidney and heart were collected and observed on an *In Vivo* Imaging System Lumina II (PerkinElmer, Waltham, MA, USA) in the fluorescent imaging mode (excitation peak = 490 nm, emission peak = 518 nm). After subtracting the background fluorescence with Living Image 4.2 (PerkinElmer), the average radiant efficiency values of these organs were measured and analyzed.

Immunofluorescence staining

After observation with the *In Vivo* Imaging System Lumina II, the brains were fixed in 4% paraformaldehyde overnight at 4°C, and then dehydrated, cleared and embedded in paraffin. The tissue blocks were sliced into 5-µm sections using a Slicer microtome (Leica Biosystems, Buffalo Grove, IL, USA). The brain sections were dewaxed, rehydrated, and placed into microwave-heated citrate buffer (pH 6.0) to retrieve the antigens at high heat for 3 minutes and medium heat for 2 minutes, and then cooled to room temperature. Sections were then rinsed three times in PBS for 10 minutes and incubated for 1 hour at room temperature in blocking solution (5% bovine serum albumin in PBS). The sections were thereafter incubated overnight at 4°C with primary antibodies, including rabbit anti-human CD29 polyclonal antibody (Cat# PB9086, 1:100, Boster), proliferating cell nuclear antigen (PCNA) mouse monoclonal antibody (Cat# 2586S, 1:4000, CST, Danvers, MA, USA), Caspase 3 (CASP3) rabbit polyclonal antibody (Cat# 19677-1-AP, 1:200, Proteintech) and F4/80 rabbit polyclonal antibody (Cat# 28463-1-AP, 1:200, Proteintech), diluted in 1% bovine serum albumin containing PBS. Then, after three rinses in PBS, the corresponding secondary antibody, CoraLite594-conjugated goat anti-rabbit IgG (Cat# SA00013-4, 1:200, Proteintech) or CoraLite594-conjugated goat anti-mouse IgG (Cat# SA00013-3, 1:200, Proteintech) was added to the sections and incubated at 37°C for 30 minutes. The sections were rinsed in PBS before incubation in 4′,6-diamidine-2′-phenylindole dihydrochloride (Cat# 10236276001, Roche) at room temperature for 5 minutes, and then mounted with 50% glycerol/PBS and imaged under a fluorescence microscope (BX51, Olympus, Shinjuku, Japan).

Immunohistochemistry

The paraffin tissue blocks were sliced into 5-µm sections and then dewaxed and rehydrated. After immersion in 3% hydrogen peroxide for 10 minutes, sections were placed into microwave-heated citrate buffer (pH 6.0) to retrieve the antigens at high heat for 3 minutes and medium heat for 2 minutes, and then cooled to room temperature. Sections were then rinsed three times in PBS for 10 minutes and incubated for 1 hour at room temperature in blocking solution (5% bovine serum albumin in PBS). The sections were subsequently incubated with epidermal growth factor receptor variant III (EGFRvIII) rabbit monoclonal antibody (Cat# 64952S, 1:100, CST), diluted in PBS containing 1% bovine serum albumin, at 4°C overnight. The next morning, the sections were rinsed three times in PBS and incubated with biotin-labeled goat anti-rabbit IgG (Cat# BA1003, 1:200, Boster), diluted in PBS, at 37°C for 30 minutes. The sections were rinsed three times in PBS, incubated with streptavidin-biotin complex (Cat# SA2002, Boster) at 37°C for 30 minutes, rinsed four times in PBS, developed with diaminobenzidine, stained with hematoxylin, mounted with neutral balsam, and imaged under a fluorescence microscope.

Hematoxylin and eosin staining

After observation under the *In Vivo* Imaging System Lumina II, the liver and lung tissues were processed into paraffin tissue blocks and sliced into 5-µm sections for hematoxylin and eosin staining. Briefly, sections were dewaxed, rehydrated and incubated with hematoxylin for 5 minutes, then rinsed with water before incubation with eosin for 30 seconds. Finally, sections were mounted with neutral balsam and photographed under a fluorescence microscope.

Statistical analysis

Statistical analysis was performed using IBM SPSS Statistics version 22.0 (IBM, Armonk, NY, USA). The concentration of inflammatory factors and average radiant efficiency values of brains/livers/lungs were compared by one-way analysis of variance followed by the least significant difference test. Repeated measures analysis of variance was used to explore the changes of concentrations of inflammatory factors at different points. $P < 0.05$ was considered statistically significant.

Results

Morphologic and immunophenotypic characteristics of huMSCs

The third passage huMSCs had a morphology resembling long whirling spindles (**Figure 1A**). Flow cytometry revealed that cells expressing CD29, CD44, CD73 and CD105 accounted for more than 95% of the total cell population (**Figure 1B**), indicating that these were indeed huMSCs, and therefore suitable for use in the following experiments.

Western blot analysis showed that no HLAII protein was expressed in the huMSCs (**Figure 1C** and **D**). qRT-PCR showed no expression of *HLA-DRA1*. While *HLA-DPA1* and *HLA-DQA1* were detected in the huMSCs (**Figure 1E** and **F**), the cycle thresholds were ~32 for these cells, compared with 24 for peripheral blood mononuclear cells. These results suggest that huMSC therapy might be immunologically tolerated.

Immunomodulatory effects of huMSCs in TBI model rats

We examined the levels of serum proinflammatory cytokines (IL-6, IL-12 and TNF-α) and anti-inflammatory cytokines (IL-10 and TGFβ) in experimental animals with ELISA. The levels of serum pro- and anti-inflammatory cytokines in the TBI model group were higher than those in the Sham group ($P < 0.001$). In the *In Situ* (huMSCs delivered *in situ* at the lesion site) and Tail Vein groups (huMSCs delivered through the tail vein), we found that the levels of proinflammatory cytokines were decreased, and the levels of anti-inflammatory cytokines were increased compared with the TBI group ($P < 0.001$; **Figure 1G**). Repeated measures analysis of variance was used to examine the changes in serum inflammatory factor concentrations in each group. Compared with the Sham group, the levels of TNF-α and IL-6 in the TBI group were significantly higher during the entire experimental observation period ($P < 0.05$). The concentrations of IL-12 and IL-10 were significantly higher in the first 7 days ($P < 0.05$), but there were no significant differences after day 14. In the Tail Vein group, the levels of pro-inflammatory cytokines were decreased significantly ($P < 0.05$) a short time after huMSC transplantation (IL-6: 3 days later, IL-12: 1 day later, and TNF-α: 3 days later). The immunomodulatory effects of the injected huMSCs persisted during the whole experimental period, such that there were no significant differences in pro-inflammatory cytokine levels between the Tail Vein and Sham groups. However, it took a longer time (IL-6: 28 days; IL-12: 3 days and TNF-α: 3 days) for injected huMSCs in the *In Situ* group to exert immunomodulatory effects. There were no statistically significant differences in pro-inflammatory cytokine levels between the *In Situ* and Tail Vein groups ($P > 0.05$).

Organ distribution of injected huMSCs in TBI model rats

Compared with the TBI group, the fluorescence intensity of the brain observed using the small animal live imager was significantly higher on days 1 and 3 in the *In Situ* group ($P < 0.001$; **Figure 2A** and **B**). However, there was no significant difference in the fluorescence intensity of the other organs (liver, lung, heart and kidney) between the TBI and *In Situ* groups (**Figure 2B**). These results indicate that the huMSCs injected into the brain injury site were primarily localized within the brain, and almost no huMSCs entered the blood from the injured brain tissue. Although the fluorescence gradually faded, it could still be seen on day 7, which might indicate that some huMSCs persist for up to a week and have adequate time to secrete regulatory factors before they undergo apoptosis or differentiate.

Compared with the TBI group, live images of the tail vein group showed fluorescence in the liver, but only weak green fluorescence in the brain, lung, heart and kidney (**Figure 2A**), indicating that the huMSCs injected into the tail vein primarily accumulated in the liver, with only a few cells making their way to the brain, lung and other organs. In addition, the fluorescence intensity of the lungs on days 1 ($P < 0.001$) and 3 ($P < 0.001$) and the fluorescence intensity of the liver on days 1 ($P < 0.001$), 3 ($P < 0.001$) and 7 ($P < 0.05$) were significantly higher in the tail vein group compared with the TBI group (**Figure 2C**). Over time, fluorescence values diminished to nearly normal levels by day 14.

Brain sections from the *In Situ* and Tail Vein groups were used to observe the location of huMSCs and the aggregation of cells under a fluorescence microscope. Considering that the fluorescence intensity of CFSE labeled huMSCs was halved once per generation, we chosed CD29, a surface molecule makers of huMSC, for immunofluorescence staining to track the transplanted huMSCs. The CFSE and CD29 labeled huMSCs were identified in the *In Situ* group and CD29 on days 1, 3 and 7 (**Figure 2D**) in the brain lesions. A few CFSE-labeled huMSCs in the Tail Vein group were also observed in the brain lesions on days 1 and 3 (**Figure 2E**).

Evaluation of tumorigenesis following huMSC transplantation in TBI model rats

The experimental rats from both the *In Situ* and Tail Vein groups exhibited no cell degeneration, necrosis, hyperplasia or tumorigenesis in the primary organs, including the liver and lungs, on days 1, 3, 7, 14 and 28, or even 12 months post-transplantation (**Figures 3A** and **4A**). Immunohistochemistry for EGFRvIII in the brain showed no positive signal in huMSC-treated rats from the day of injection to 12 months after injection in either group (**Figures 3B** and **4B**). As EGFRvIII is one of the most common carcinogenic mutations in glioma (Kim et al., 2021), these results provide additional assurance to their clinical application.

Furthermore, immunofluorescence staining of PCNA showed that TBI triggered the proliferative activity of adjacent neurocytes, but the fluorescently labeled huMSCs had no proliferative activity in the brain lesion sites in either the *In Situ* group (**Figure 3C**) or Tail Vein group (**Figure 4C**). These results demonstrate that uncontrolled proliferation of transplanted huMSCs did not occur, even 12 months after transplantation.

Fate analysis of injected huMSCs in the brains of TBI rats

We also performed immunofluorescence staining for CASP3 and F4/80 in the brains of rats from both the *In Situ* and Tail Vein groups. In CFSE-labeled huMSCs, CASP3 was observed from days 3 to 7 in both groups (**Figure 5A** and **C**). Although no CFSE-labeled huMSCs were found after day 14, CASP3 immunoreactivity persisted until day 28, which may have resulted from apoptosis of damaged neurons. Immunostaining for F4/80, a unique marker of murine macrophages (Dos Anjos Cassado, 2017), showed that macrophages aggregated near the lesion site after huMSC injection (**Figure 5B** and **D**). Notably, the number of macrophages in the *In Situ* group (**Figure 5B**) was greater than that in the Tail Vein group (**Figure 5D**), especially on day 14.

Discussion

The current management of TBI is mainly supportive, with much more attention given to intensive care and prevention of secondary neopathy. Numerous recent studies have found that MSCs, with their multipotency and low immunogenicity, have potential in treating TBI (Cox et al., 2019; Das et al., 2019; Zhou et al., 2019; Bonsack et al., 2020; Dehghanian et al., 2020; Schepici et al., 2020; Sun et al., 2021). However, a number of issues related to the potential risk of huMSC-based therapies remain unresolved, such as the purity and identity of huMSCs, the risk of tumor formation, unwanted immune responses, and adventitious infection (Herberts et al., 2011; Das et al., 2019). In this study, our findings from both *in vitro* and *in vivo* preclinical studies suggest that huMSCs do not display immunogenic toxicity or tumorigenicity up to 12 months after implantation. Furthermore, huMSCs exhibit good immunomodulatory function by decreasing pro-inflammatory cytokine concentrations and increasing anti-inflammatory cytokine levels *in vivo*, which may play an important role in controlling inflammatory responses after TBI.

Compared with bone marrow-derived MSCs, huMSCs have similar proliferative and multi-lineage differentiation potentials (Baksh et al., 2007), but have many advantages, such as a wide variety of sources, easy harvesting, less risk

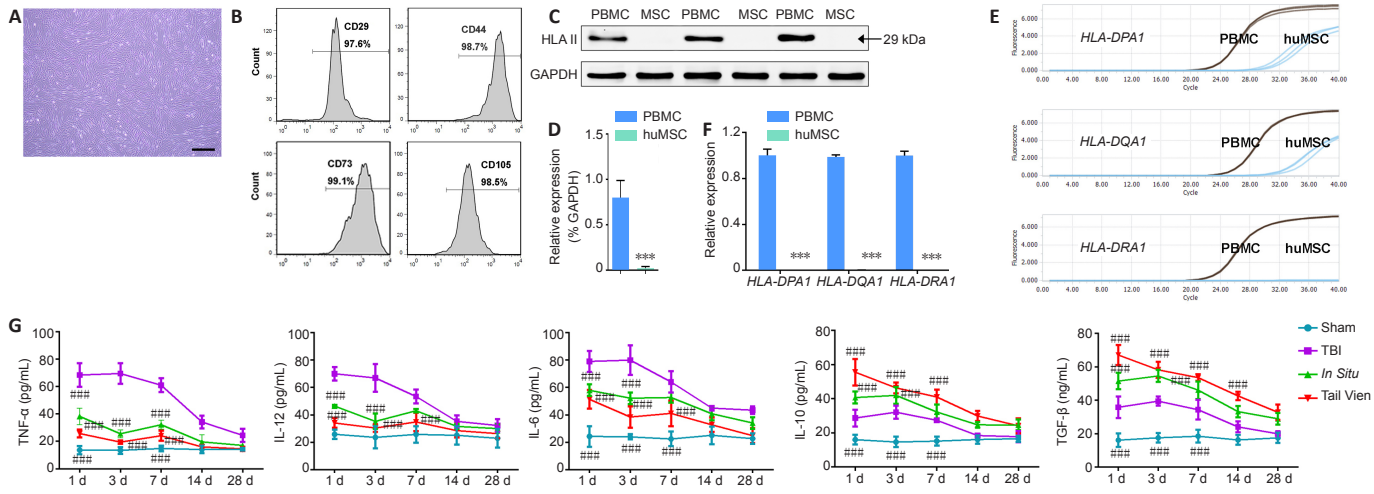

Figure 1 | **Identification, immunogenicity and immunomodulation of huMSCs.**

(A) The huMSCs cultured in our experiment. The huMSCs were spindle-shaped and grew in a whorl pattern. Original magnification 100×, scale bars: 200 μm. (B) Flow cytometry detection of CD29, CD44, CD73 and CD105. The rate of positive expression for all factors was greater than 95%. (C) Detection of huMSC HLAII expression in PBMCs and huMSCs by western blot. No HLAII expression band was detected in the huMSCs. (D) Relative expression of HLAII in PBMCs and huMSCs. The bar graph shows no HLAII expression in huMSCs. (E) PCR amplification curves of *HLA-DPA1*, *HLA-DQA1* and *HLA-DRA1* genes in PBMCs and huMSCs. (F) Relative expression of *HLA-DPA1*, *HLA-DQA1* and *HLA-DRA1* genes in PBMCs and huMSCs. PCR results showed no expression of *HLA-DPA1*, *HLA-DQA1* or *HLA-DRA1* genes in huMSCs. (G) Expression curves of serum IL-6, IL-10, IL-12, TGF-β, and TNF-α detected by ELISA method (n = 5 rats per group). Compared with the TBI group, the serum pro-inflammatory cytokines IL-6, IL-12 and TNF-α in the Tail Vein and *In Situ* group were lower (###P < 0.001), whereas the inflammation inhibiting factors IL-10 and TGF-β were much higher (###P < 0.001), indicating that huMSCs exert good immunoregulatory effects. Data are expressed as the mean ± SD. ***P < 0.001, *vs*. PBMCs (one-way analysis of variance followed by least significant difference test). ELISA: Enzyme-linked immunosorbent assay; GAPDH: glyceraldehyde 3-phosphate dehydrogenase; HLAII: human leukocyte antigen II; huMSCs: human umbilical cord mesenchymal stem cells; IL: interleukin; PBMCs: peripheral blood mononuclear cells; PCR: polymerase chain reaction; TBI: traumatic brain injury; TGF-β: transforming growth factor beta; TNF-α: tumor necrosis factor alpha.

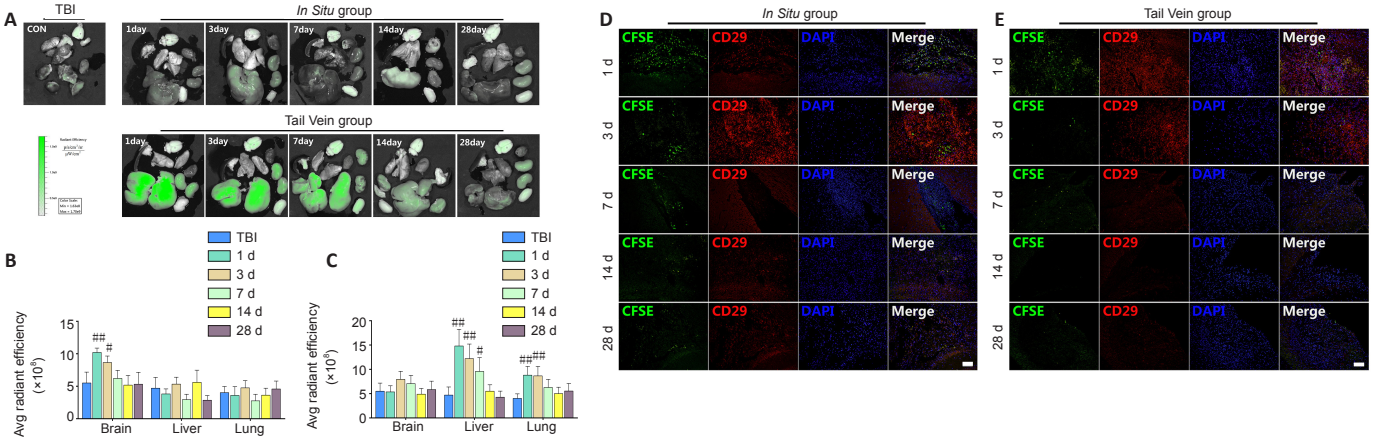

Figure 2 | **Sites of accumulation of huMSCs *in vivo* in TBI rats.**

(A) Live imaging of the primary organs of experimental rats. (B, C) The average fluorescence intensity in the brain, liver and lung in the *In Situ* (B) and Tail Vein (C) groups. Data are expressed as the mean ± SD (n = 5 rats at each time point). #P < 0.05, ##P < 0.01, *vs*. TBI group (one-way analysis of variance followed by least significant difference test). (D, E) CD29 (red, stained by CoraLite594) immunoreactivity in CFSE-labeled huMSCs in brain tissue (immunofluorescence staining, original magnification 200×, scale bars: 100 μm). CD29 and CFSE co-labeled huMSCs were identified in the In Situ group on days 1, 3 and 7 (D) in the brain lesions. A few CFSE-labeled huMSCs in the Tail Vein group were also observed in the brain lesions on days 1 and 3 (E). CFSE: Carboxyfluorescein succinimidyl ester; CON: TBI group; DAPI: 4′,6-diamidine-2′-phenylindole dihydrochloride; huMSCs: human umbilical cord mesenchymal stem cells; TBI: traumatic brain injury.

of rejection after transplantation, low immunogenicity, and no ethical controversy. Therefore, huMSCs are considered an ideal alternative to bone marrow-derived MSCs. However, efficiently isolating huMSCs from human umbilical cord tissues and identifying them remain key tasks for the development of huMSC-based therapies. Currently, MSC isolation/identification has mainly relied on surface markers detected by flow cytometry, adherent properties, and differentiation potential (Bernardo et al., 2009). Our results show that the third passage huMSCs have a morphology resembling long whirling spindles. Flow cytometry revealed that cells with characteristic expression of CD29, CD44, CD73 and CD105 accounted for more than 95% of the total cell population, indicating that our protocol for huMSC isolation and identification was appropriate, guaranteeing the purity of huMSCs for experiments. This is another advantage of huMSCs over bone marrow-derived MSCs, as the latter contain multiple types of stem cells, such as hematopoietic stem cells, which can cause undesirable effects. To be defined as MSCs, cells must be positive for a number of surface markers, such as CD73, CD90, CD166, CD44 and CD29. Furthermore, they must be negative for CD34, CD31, CD14 and CD45 (at least in case of BM-derived cells), as well as HLA complex surface molecules (Le Blanc et al., 2003). The HLA complex, also called the HLA gene complex, is primarily located on chromosome 6p21, encoding the MHC cell-surface antigens responsible

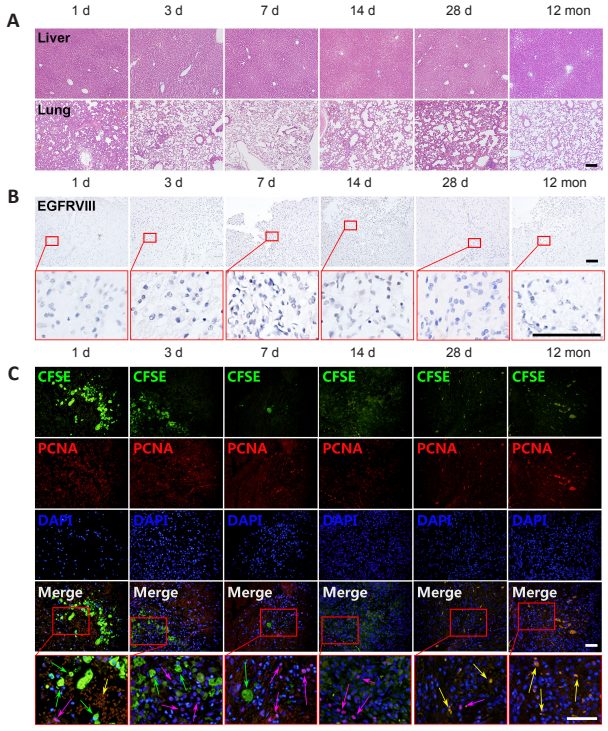

Figure 3 | Evaluation of tumorigenicity in TBI rats given *in situ* huMSC transplantation.
(A) Pathology of livers and lungs in the *In Situ* group (original magnification 100×). Scale bar: 200 μm. No cell degeneration, necrosis, hyperplasia or tumorigenesis was observed in the liver and lungs on days 1, 3, 7, 14 or 28, or even 12 months post-transplantation. (B) Immunohistochemical staining for EGFRvIII in the *In Situ* group (original magnification 200×). Scale bar: 100 μm. No positive signal was observed in huMSC-treated rats from the day of injection to 12 months after injection. (C) Immunofluorescence staining for PCNA in the *In Situ* group (original magnification 400×). Scale bar: 50 μm. There was no PCNA immunoreactivity (positive signal) in CFSE-labeled huMSCs (green arrows), indicating that the huMSCs do not exhibit proliferative activity. However, the adjacent neural cells are PCNA-positive (red, stained by CoraLite594, pink arrows) due to the responsive proliferation of gliocytes and nerve cells after brain injury. The cells indicated by yellow arrows are red cells that exhibit autofluorescence. CFSE: Carboxyfluorescein succinimidyl ester; EGFRvIII: epidermal growth factor receptor variant III; huMSCs: human umbilical cord mesenchymal stem cells; PCNA: proliferating cell nuclear antigen; TBI: traumatic brain injury.

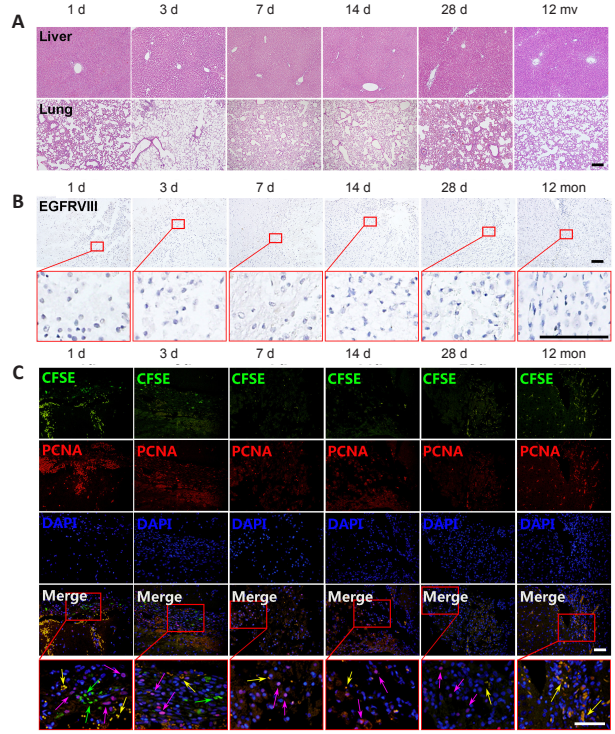

Figure 4 | Evaluation of tumorigenicity in TBI rats given huMSC transplantation via tail vein injection.
(A) Pathology of the liver and lung in the Tail Vein group (original magnification 100×). Scale bar: 200 μm. No cell degeneration, necrosis, hyperplasia or tumorigenesis was observed in the liver or lungs, on days 1, 3, 7, 14 or 28, or even 12 months post-transplantation. (B) Immunohistochemistry for EGFRvIII in the Tail Vein group (original magnification 200×). Scale bar: 100 μm. No positive signal was observed in huMSC-treated rats from the day of injection to 12 months after injection. (C) Immunofluorescence staining for PCNA in the Tail Vein group (original magnification 400×). Scale bar: 50 μm. The results are consistent with those of the *In Situ* group. There was no PCNA immunoreactivity (positive signal) in CFSE-labeled huMSCs (indicated by green arrows), indicating that the huMSCs do not exhibit proliferative activity. However, the adjacent neural cells show PCNA immunoreactivity (red, stained by CoraLite594, pink arrows) caused by the responsive proliferation of glia and neuronal cells after brain injury. The cells indicated by yellow arrows are red cells that exhibit autofluorescence. CFSE: Carboxyfluorescein succinimidyl ester; EGFRvIII: epidermal growth factor receptor variant III; huMSCs: human umbilical cord mesenchymal stem cells; PCNA: proliferating cell nuclear antigen; TBI: traumatic brain injury.

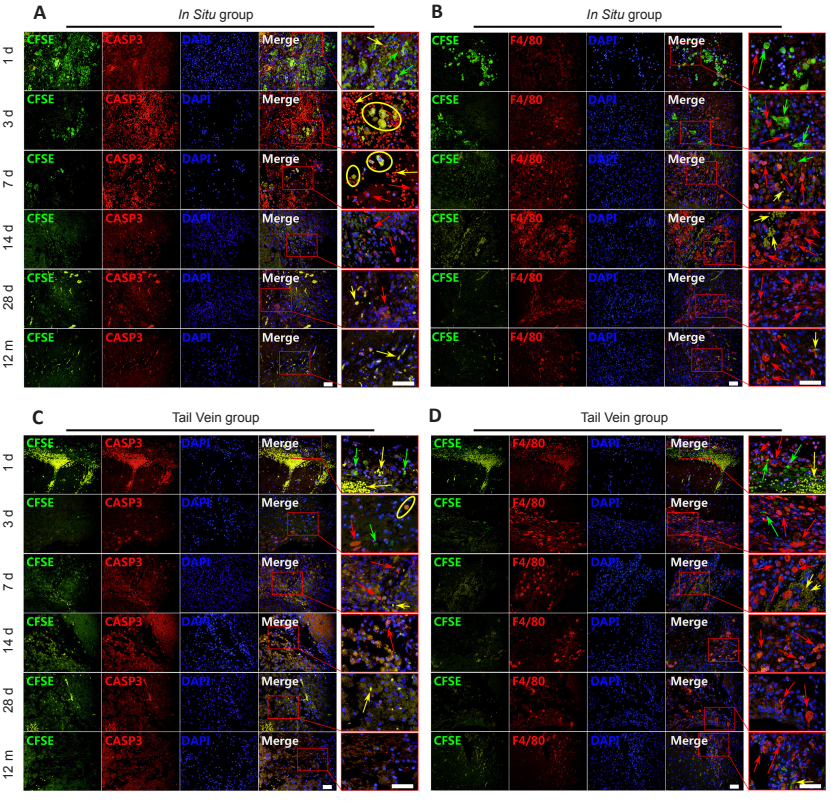

Figure 5 | The fate of huMSCs in TBI rats given *in situ* or tail vein transplantation.
(A) Fluorescence staining of CASP3 in the *In Situ* group. On the first day after the last transplantation, there was no immunoreactivity towards CASP3 (red, stained by CoraLite594, red arrows) in huMSCs (green arrows). huMSCs began to express caspase 3 (denoted by a yellow ellipse) from the third day post final transplantation, indicating that huMSCs began to undergo apoptosis. On the 14th day, almost no huMSCs remained. The neural cells in the injury site can also undergo apoptosis as they express CASP3. (B) Fluorescence staining for F4/80 (red, stained by CoraLite594) in the *In Situ* group. On the first day after injection of huMSCs, there were some macrophages (red, red arrows) around the CFSE-labeled huMSCs (indicated by green arrows). Over time, more macrophages accumulated, and they persisted up to 12 months later. (C) Fluorescence staining results of CASP3 in the Tail Vein group are similar to those in the *In Situ* group. (D) Fluorescence staining results of F4/80 in the Tail Vein group are similar to those in the *In Situ* group. However, the number of macrophages in the Tail Vein group was less than that in the *In Situ* group, especially on the 14th day. Cells indicated by yellow arrows are red cells that exhibit autofluorescence (original magnification 400×, scale bar: 50 μm). CASP3: Caspase 3; CFSE: carboxyfluorescein succinimidyl ester; huMSCs: human umbilical cord mesenchymal stem cells; TBI: traumatic brain injury.

for graft-versus-host disease and transplant rejection. There are three major categories of HLAs: MHC class I (A, B and C), MHC class II (DP, DM, DOA, DOB, DQ and DR), and MHC class III. MHC class II plays the major role of presenting antigens on the surface to T-lymphocytes (Tan et al., 2017). In our study, we found that the huMSCs expressed no MHC class II antigens, making them unable to present host antigens to the T-cells. Therefore, the problems of graft-versus-host disease or transplant rejection can be mitigated by huMSC therapy.

A molecular war begins between anti-inflammatory and pro-inflammatory cytokines after TBI (Helmy et al., 2011a). Pro-inflammatory cytokines, including IL-6, IL-12 and TNF-α, which are mainly produced by microglia, but also by endothelial cells, neurons and astrocytes, activate glial cells, inducing further cytokine production and astrogliosis (Lau and Yu, 2001; Konsman et al., 2007; Ziebell and Morganti-Kossmann, 2010). Anti-inflammatory cytokines such as TGF-β and IL-10 have the ability to counteract and downregulate inflammatory and cytotoxic reactions (Cederberg and Siesjö, 2010). It was reported that pro-inflammatory cytokines are rapidly upregulated following brain injury, and some peak as early as 2 hours after TBI (Helmy et al., 2011b). These pro-inflammatory cytokines stimulate the injected huMSCs to exhibit an immunosuppressive effect (Ren et al., 2008). Our results show that levels of serum pro-inflammatory cytokines (IL-6, IL-12 and TNFα) and anti-inflammatory cytokines (IL-10 and TGF-β) in the TBI model group were higher than those in the sham group. Significantly decreased pro-inflammatory cytokine levels and increased anti-inflammatory cytokine levels were observed shortly after huMSCs transplantation, in agreement with another study (Zhang et al., 2013). In that study, IL-6 at 24 and 72 hours, and TNF-α at 24 and 72 hours were all significantly decreased in the MSC-treated group compared with the control group. Moreover, levels of the anti-inflammatory cytokines IL-10 at 24 and 72 hours, and TGF-β at 24 and 72 hours after TBI were increased in the MSC-treated group compared with the control group. The benefit of stem cell therapy for TBI may primarily arise from the paracrine or systemic secretion of anti-inflammatory chemokines and various growth factors, and by the inhibition of pro-inflammatory cytokines, rather than their differentiation into neural cells (Uccelli et al., 2008; Scuteri et al., 2011; Lo Sicco et al., 2017).

Since the fluorescence of CFSE labeled cells is halved every generation, immunofluorescence staining of CD29, a surface molecule maker of huMSCs, was implemented to batter track the transplanted huMSCs. CFSE and CD29 co-localization in brain sections, combined with live images, showed the presence of huMSCs in brain tissue during the first week during which huMSCs secrete anti-inflammatory chemokines and various growth factors to repair brain tissue. Because of the apoptosis or differentiation of huMSCs, the fluorescence gradually decreased, and was metabolized primarily in the liver in our study. EGFRvIII, which is a specific EGFR mutation, is often used to detect brain tumors (Kuan et al., 2001; Gong et al., 2014). PCNA is a DNA clamp that acts as a processivity factor for DNA polymerase δ in eukaryotic cells and is essential for replication. PCNA is expressed in the nuclei of cells during the DNA synthesis phase of the cell cycle, and its abnormal increase is related to certain neoplasms, such as breast carcinomas and astrocytomas (Leonardi et al., 1992). Imaging of antibody labeling for PCNA can be used to distinguish the early, mid and late S phase of the cell cycle (Schönenberger et al., 2015). Neither expression of EGFRvIII nor PCNA increased, even 12 months post-transplantation, which aligns with another study that evaluated the tumorigenicity of transplanted stem cells (Garitaonandia et al., 2016). However, the follow-up time of that study was 9 months.

The routes of delivering stem cells to the host, which commonly include intravenous, intra-arterial and intracranial delivery methods, play an important role in the success of stem cell therapies. The intravenous method seems to be the most attractive for clinical applications, whereas the intracranial method is the most frequently used. When we designed our study, two groups, the *In Situ* and Tail Vein groups, were created to allow a direct comparison of the two delivery methods. Some interesting results are worth noting. The huMSCs injected into the Tail Vein group primarily accumulated in the liver, while those in the *In Situ* group primarily accumulated in the brain, which was expected. Additionally, our results indicated that huMSC injection increased levels of serum anti-inflammatory cytokines and decreased the concentrations of pro-inflammatory cytokines in rats with TBI. However, there were no statistically significant differences in pro-inflammatory cytokine levels between the *In Situ* and Tail Vein groups. Third, the number of macrophages was greater in the *In Situ* group than in the Tail Vein group. Macrophages are important cells of the immune system that respond to an infection or to the accumulation of damaged or dead cells. Injected huMSCs gradually undergo apoptosis and might be cleared away by macrophages.

There are some limitations to this study. First, some biological properties, such as population doubling time, clonogenicity, and differentiation ability of the huMSCs were not examined. Second, only CD29, CD44, CD73 and CD105 were assayed. Third, we focused on the safety evaluation of the injected huMSCs, but not on efficacy assessment. It would have been informative to examine whether the transplanted huMSCs differentiated into glial cells, such as astrocytes or oligodendrocytes, or into neuron-like cells by co-labeling for the appropriate markers, *in vivo* and *in vitro*. Furthermore, it would have been interesting to explore whether the huMSCs could have differentiated into macrophage-like cells. It could have provided information on their immunoregulatory role, particularly as some classes of macrophages can reduce inflammation.

In summary, in this study, we comprehensively evaluated the safety of huMSCs for treating TBI in rats, and the findings suggest that allogeneic huMSC therapy may be a good strategy for treating TBI without major risk of immune attack or rejection. Given the encouraging safety data obtained in this study, we propose further efficacy evaluation of huMSCs for human application.

Author contributions: *Study design, data analysis and interpretation, manuscript review: BD; animal, ELISA, live imaging, and slice experiments, data collecting and assembling, manuscript writing: DQY, HLW, YPL, GW; PCR and western blot assay: ZLY, LC; cell experiment: QY, YSG. All authors contributed to this study and approved the final manuscript.*
Conflicts of interest: *All the authors have declared that they have no competing interests.*
Financial support: *The work was supported by the General Project of Hubei Health Committee of China, No. WJ2019M263 (to GW). The funder had no roles in the study design, conduction of experiment, data collection and analysis, decision to publish, or preparation of the manuscript.*
Institutional review board statement: *The study was approved by the Ethics Committee of Wuhan General Hospital of PLA (approval No. 20160054) on November 1, 2016.*
Declaration of patient consent: *The authors certify that they have obtained the consent forms from the donor. In the form, the donor has given her consent for the images and other clinical information to be reported in the journal. The donor understand that her name and initials will not be published.*

Data sharing statement: *Datasets analyzed during the current study are available from the corresponding author on reasonable request.*
Plagiarism check: *Checked twice by iThenticate.*
Peer review: *Externally peer reviewed.*

Open peer reviewers: *Elena Abati, Facolta di Medicina e Chirurgia, Italy; Fei Gao, University of Pittsburgh, USA.*
Additional file: *Open peer review reports 1 and 2.*

References

Baksh D, Yao R, Tuan RS (2007) Comparison of proliferative and multilineage differentiation potential of human mesenchymal stem cells derived from umbilical cord and bone marrow. Stem Cells 25:1384-1392.
Bernardo ME, Locatelli F, Fibbe WE (2009) Mesenchymal stromal cells. Ann N Y Acad Sci 1176:101-117.
Blaya MO, Tsoulfas P, Bramlett HM, Dietrich WD (2015) Neural progenitor cell transplantation promotes neuroprotection, enhances hippocampal neurogenesis, and improves cognitive outcomes after traumatic brain injury. Exp Neurol 264:67-81.
Bonsack B, Corey S, Shear A, Heyck M, Cozene B, Sadanandan N, Zhang H, Gonzales-Portillo B, Sheyner M, Borlongan CV (2020) Mesenchymal stem cell therapy alleviates the neuroinflammation associated with acquired brain injury. CNS Neurosci Ther 26:603-615.
Cederberg D, Siesjö P (2010) What has inflammation to do with traumatic brain injury? Childs Nerv Syst 26:221-226.
Cox CS, Jr., Juranek J, Bedi S (2019) Clinical trials in traumatic brain injury: cellular therapy and outcome measures. Transfusion 59:858-868.
Das M, Mayilsamy K, Mohapatra SS, Mohapatra S (2019) Mesenchymal stem cell therapy for the treatment of traumatic brain injury: progress and prospects. Rev Neurosci 30:839-855.
Dehghanian F, Soltani Z, Khaksari M (2020) Can mesenchymal stem cells act multipotential in traumatic brain injury? J Mol Neurosci 70:677-688.
Dos Anjos Cassado A (2017) F4/80 as a major macrophage marker: the case of the peritoneum and spleen. Results Probl Cell Differ 62:161-179.
Feeney DM, Boyeson MG, Linn RT, Murray HM, Dail WG (1981) Responses to cortical injury: I. Methodology and local effects of contusions in the rat. Brain Res 211:67-77.
Gao J, Grill RJ, Dunn TJ, Bedi S, Labastida JA, Hetz RA, Xue H, Thonhoff JR, DeWitt DS, Prough DS, Cox CS, Jr., Wu P (2016) Human neural stem cell transplantation-mediated alteration of microglial/macrophage phenotypes after traumatic brain injury. Cell Transplant 25:1863-1877.
Garitaonandia I, Gonzalez R, Christiansen-Weber T, Abramihina T, Poustovoitov M, Noskov A, Sherman G, Semechkin A, Snyder E, Kern R (2016) Neural stem cell tumorigenicity and biodistribution assessment for phase i clinical trial in Parkinson's disease. Sci Rep 6:34478.
Gong H, Kovar JL, Cheung L, Rosenthal EL, Olive DM (2014) A comparative study of affibody, panitumumab, and EGF for near-infrared fluorescence imaging of EGFR- and EGFRvIII-expressing tumors. Cancer Biol Ther 15:185-193.
Helmy A, Carpenter KL, Menon DK, Pickard JD, Hutchinson PJ (2011a) The cytokine response to human traumatic brain injury: temporal profiles and evidence for cerebral parenchymal production. J Cereb Blood Flow Metab 31:658-670.
Helmy A, De Simoni MG, Guilfoyle MR, Carpenter KL, Hutchinson PJ (2011b) Cytokines and innate inflammation in the pathogenesis of human traumatic brain injury. Prog Neurobiol 95:352-372.
Herberts CA, Kwa MS, Hermsen HP (2011) Risk factors in the development of stem cell therapy. J Transl Med 9:29.
Kim HM, Lee SH, Lim J, Yoo J, Hwang DY (2021) The epidermal growth factor receptor variant type III mutation frequently found in gliomas induces astrogenesis in human cerebral organoids. Cell Prolif 54:e12965.
Konsman JP, Drukarch B, Van Dam AM (2007) (Peri)vascular production and action of pro-inflammatory cytokines in brain pathology. Clin Sci (Lond) 112:1-25.
Kuan CT, Wikstrand CJ, Bigner DD (2001) EGF mutant receptor vIII as a molecular target in cancer therapy. Endocr Relat Cancer 8:83-96.
Lam PK, Wang KKW, Lo AWI, Tong CSW, Ching DWC, Wong K, Yang Z, Kong T, Lo KKY, Choy RKW, Lai PBS, Wong GKC, Poon WS (2017) Interactome and reciprocal activation of pathways in topical mesenchymal stem cells and the recipient cerebral cortex following traumatic brain injury. Sci Rep 7:5017.
Lau LT, Yu AC (2001) Astrocytes produce and release interleukin-1, interleukin-6, tumor necrosis factor alpha and interferon-gamma following traumatic and metabolic injury. J Neurotrauma 18:351-359.
Le Blanc K, Tammik C, Rosendahl K, Zetterberg E, Ringdén O (2003) HLA expression and immunologic properties of differentiated and undifferentiated mesenchymal stem cells. Exp Hematol 31:890-896.
Leonardi E, Girlando S, Serio G, Mauri FA, Perrone G, Scampini S, Dalla Palma P, Barbareschi M (1992) PCNA and Ki67 expression in breast carcinoma: correlations with clinical and biological variables. J Clin Pathol 45:416-419.
Liu S, Xie YY, Wang LD, Tai CX, Chen D, Mu D, Cui YY, Wang B (2021) A multi-channel collagen scaffold loaded with neural stem cells for the repair of spinal cord injury. Neural Regen Res 16:2284-2292.
Lo Sicco C, Reverberi D, Balbi C, Ulivi V, Principi E, Pascucci L, Becherini P, Bosco MC, Varesio L, Franzin C, Pozzobon M, Cancedda R, Tasso R (2017) Mesenchymal stem cell-derived extracellular vesicles as mediators of anti-inflammatory effects: endorsement of macrophage polarization. Stem Cells Transl Med 6:1018-1028.
Nakamura K, Ito Y, Kawano Y, Kurozumi K, Kobune M, Tsuda H, Bizen A, Honmou O, Niitsu Y, Hamada H (2004) Antitumor effect of genetically engineered mesenchymal stem cells in a rat glioma model. Gene Ther 11:1155-1164.
Ren G, Zhang L, Zhao X, Xu G, Zhang Y, Roberts AI, Zhao RC, Shi Y (2008) Mesenchymal stem cell-mediated immunosuppression occurs via concerted action of chemokines and nitric oxide. Cell Stem Cell 2:141-150.
Saatman KE, Duhaime AC, Bullock R, Maas AI, Valadka A, Manley GT (2008) Classification of traumatic brain injury for targeted therapies. J Neurotrauma 25:719-738.
Schepici G, Silvestro S, Bramanti P, Mazzon E (2020) Traumatic brain injury and stem cells: an overview of clinical trials, the current treatments and future therapeutic approaches. Medicina (Kaunas) 56:137.
Schönenberger F, Deutzmann A, Ferrando-May E, Merhof D (2015) Discrimination of cell cycle phases in PCNA-immunolabeled cells. BMC Bioinformatics 16:180.
Scuteri A, Miloso M, Foudah D, Orciani M, Cavaletti G, Tredici G (2011) Mesenchymal stem cells neuronal differentiation ability: a real perspective for nervous system repair? Curr Stem Cell Res Ther 6:82-92.
Shi W, Nie D, Jin G, Chen W, Xia L, Wu X, Su X, Xu X, Ni L, Zhang X, Zhang X, Chen J (2012) BDNF blended chitosan scaffolds for human umbilical cord MSC transplants in traumatic brain injury therapy. Biomaterials 33:3119-3126.
Sun C, Zhang AD, Chen HH, Bian J, Liu ZJ (2021) Magnet-targeted delivery of bone marrow-derived mesenchymal stem cells improves therapeutic efficacy following hypoxic-ischemic brain injury. Neural Regen Res 16:2324-2329.
Svensson A, Ramos-Moreno T, Eberstål S, Scheding S, Bengzon J (2017) Identification of two distinct mesenchymal stromal cell populations in human malignant glioma. J Neurooncol 131:245-254.
Tan K, Zheng K, Li D, Lu H, Wang S, Sun X (2017) Impact of adipose tissue or umbilical cord derived mesenchymal stem cells on the immunogenicity of human cord blood derived endothelial progenitor cells. PLoS One 12:e0178624.
Tyagi V, Theobald J, Barger J, Bustoros M, Bayin NS, Modrek AS, Kader M, Anderer EG, Donahue B, Fatterpekar G, Placantonakis DG (2016) Traumatic brain injury and subsequent glioblastoma development: Review of the literature and case reports. Surg Neurol Int 7:78.
Uccelli A, Moretta L, Pistoia V (2008) Mesenchymal stem cells in health and disease. Nat Rev Immunol 8:726-736.
Xu L, Ryu J, Hiel H, Menon A, Aggarwal A, Rha E, Mahairaki V, Cummings BJ, Koliatsos VE (2015) Transplantation of human oligodendrocyte progenitor cells in an animal model of diffuse traumatic axonal injury: survival and differentiation. Stem Cell Res Ther 6:93.
Yuan CH, Cui ZZ, Wu D (2021) Meta-analysis of autologous bone marrow mesenchymal stem cell transplantation in the treatment of ischemic stroke. Zhongguo Zuzhi Gongcheng Yanjiu 25:5018-5024.
Zhang R, Liu Y, Yan K, Chen L, Chen XR, Li P, Chen FF, Jiang XD (2013) Anti-inflammatory and immunomodulatory mechanisms of mesenchymal stem cell transplantation in experimental traumatic brain injury. J Neuroinflammation 10:106.
Zhou Y, Shao A, Xu W, Wu H, Deng Y (2019) Advance of stem cell treatment for traumatic brain injury. Front Cell Neurosci 13:301.
Ziebell JM, Morganti-Kossmann MC (2010) Involvement of pro- and anti-inflammatory cytokines and chemokines in the pathophysiology of traumatic brain injury. Neurotherapeutics 7:22-30.

P-Reviewers: Abati E, Gao F; C-Editor: Zhao M; S-Editors: Yu J, Li CH; L-Editors: Patel B, Yu J, Song LP; T-Editor: Jia Y